文章编号:1001-9014(2012)06-0486-05

DOI:10.3724/SP.J.1010.2012.00486

Simulation of transport properties in mid-infrared quantum cascade lasers

LI Ying-Ying[1], RU Guo-Ping[1*], LI Z.-M. Simon[2]

(1. State Key Laboratory of ASIC and System, Department of Microelectronics, Fudan University, Shanghai 200433, China;
2. Crosslight Software Inc., V5C 6P8, Canada)

Abstract: Simulation of transport properties in mid-infrared quantum cascade lasers (QCLs) with different structures at different temperatures based on non-local transport model is reported. With this model, drift-diffusion equations were solved with modification of current density by accounting for long-range carrier transport including quantum tunneling, mini-band tunneling and hot carrier transport in the device. The simulation with the above model was compared with experimental data and reasonable agreements with experiments have been obtained with some reasonable fitting parameters.

Key words: quantum cascade laser; simulation; transport properties; non-local transport model

PACS: 07.05.Tp, 42.55.Px

中红外量子级联激光器输运特性的仿真

李营营[1], 茹国平[1*], 李湛明[2]

(1. 复旦大学 微电子研究院 集成电路与系统国家重点实验室,上海 200433;
2. Crosslight 软件有限公司,加拿大,V5C 6P8)

摘要:基于一种非局域化的输运模型,对不同结构不同温度下的中红外量子级联激光器的输运特性进行了仿真。在这个模型中,利用量子隧穿、微带隧穿以及热载流子输运等长程载流子输运模型,对传统的扩散-漂移方程进行了矫正.并将基于上述集成模型的计算结果和实验结果进行了比较,通过拟合参数的合理设置,计算结果和实验结果得到了很好的吻合.

关 键 词:量子级联激光器;仿真;输运特性;非局域化输运模型

中图分类号:TN311,TN313 **文献标识码**:A

Introduction

As a complex quantum system, quantum cascade lasers (QCLs) can been modeled in various ways, from rate equation model[1-3], Monte-Carlo simulations[4-7], non-equilibrium Green´s function[8-10], to density matrix model[11-12]. Most of these theories are based on microscopic modeling scale which can only predict carrier dynamics in short range without a macroscopic consideration of long-range carrier transport in the whole device. Besides, it's clear that such types of models will be time-consuming if extended to large-period QCLs. So a numerically efficient model will be necessary to predict carrier dynamics in QCLs.

In our previous articles[13-14], a simulation study of carrier transport in mid-infrared QCLs with different periods based on non-local transport model was reported. With non-local mobility (μ_n) and mean free path (MFP λ_n) as fitting parameters, reasonable agreement was obtained at low temperature when the tunneling path from the injector ground level to the upper laser level is expected to significantly contribute to the current and the electrons excited to the continuum are negligible. However the agreement with experiment is not very good when leakage current can

Received date: 2011-12-26, **revised date**: 2012-07-04 **收稿日期**:2011-12-26, **修回日期**:2012-07-04

Foundation items: Supported by the International Research Training Group "Materials and Concepts for Interconnects and Nanosystems"

Biography: LI Ying-Ying (1985-), female, Henan, Master Candidate. Research fields focus on modeling and simulation of semiconductor devices. E-mail: 09212020028@fudan.edu.cn.

* **Corresponding author**: gpru@fudan.edu.cn.

not be ignored, for example, at high temperature. The fitting results showed that non-local mobility and MFP should scale with periods linearly.

In this paper, we will report a simulation study of transport properties of a couple of mid-infrared QCLs at different temperatures based on improved non-local transport model. This model has been implemented in LASTIP and PICS3D softwares[15]. Models and simulation methods are described in section 2, where detailed discussion of non-local transport model is shown. The simulation results and analysis are demonstrated in section 3. Conclusions made from the study are given in section 4.

1 Transport model

This model is an integration of a number of transport models on both microscopic and macroscopic scales[13]. On the microscopic scale, quantum mechanical computation was performed to find quantization states and rate equations were used to compute carrier distribution and optical gain of the device. On the macroscopic scale, as a unipolar semiconductor device, two basic equations used to govern the electrical behavior of QCLs, Poisson's equation and current continuity equation for electrons can be written as follows

$$-\nabla\left(\frac{\varepsilon_0\varepsilon_{dc}}{q}\nabla V\right) = -n + p + N_D(1-f_D) - N_A f_A + \sum_j N_{ij}(\delta_j - f_{ij}), \quad (1)$$

$$\nabla J_n - \sum R_n^{ij} - R_{sp} - R_{st} - R_{au} + G_{opt}(t) = \frac{\partial n}{\partial t} + N_D\frac{\partial f_D}{\partial t}. \quad (2)$$

The primary function of our simulator is to solve these equations self-consistently for the electrostatic potential, the electron concentrations. The carrier flux densities J_n can be written as functions of carrier concentration and the quasi-Fermi level.

$$J_n = n\mu_n \nabla E_{fn} + J_{nl}. \quad (3)$$

When using above equation, the usual boundary of thermionic emission is imposed and this ensures that thermal carriers with energy higher than a barrier or a hetro-junction can flow through to account for the thermal behavior of the device.

Last term J_{nl} is a correction to the first term, the classical drift-diffusion current. They represent long-range mechanisms such as quantum tunneling, miniband tunneling, and hot carrier transport. Such a correction is implemented as non-local transport current density flowing from mesh point i to a remote point j, which we choose according to some reasonable assumption of length scale of interaction.

In analogy to the classical Drude´s scattering model for metals[16], we assumed the general trend for hot carriers and long range tunneling decay with distance between mesh point i to j exponentially, using a characteristic MFP λ_n:

$$J_{nl} = \exp(-d_{ij}/\lambda_n)\sqrt{n_i n_j}\mu_{nl}[E_{fn}(i) - E_{fn}(i)], \quad (4)$$

where the subscripts i and j denote quantities evaluated at mesh point i and at a remote site j, respectively, and μ_{nl} are non-local mobility of carriers transporting from i to j.

According to the density matrix model reported by Terazzi *et al.*[11-12], the current density between ground state of injection and upper lasing level coupled through injection barrier can be expressed as

$$J = \frac{4q\hbar\Omega^2\gamma}{\Delta^2 + (2\gamma)^2}\{\theta(\Delta)[n_g - n_3\exp(-\beta|\Delta|)] + \theta(-\Delta)[n_g\exp(-\beta|\Delta|) - n_3]\}, \quad (5)$$

where q is elementary charge, $\hbar\Omega$ is coupling energy through the barrier, d is the difference between two centroids of the wave functions, γ is broadening of state, Δ is the detuning between subband energy, $\theta(x)$ is the Heaviside function, with $\theta(x^+) = 1$, $\theta(x^-) = 0$ and $\theta(0) = 0.5$, $\beta = 1/kT$, with k the Boltzmann constant, n_g is the net population of level g and n_3 is the net population of level 3.

Using equation above and assuming $n_g >> n_3$, the equivalent electron mobility from level g to level 3 can be expressed as

$$\mu_n = A\frac{4\hbar\Omega^2\gamma}{F[\Delta^2 + (2\gamma)^2]}[\theta(\Delta) + \theta(-\Delta)\exp(-\beta|\Delta|)], \quad (6)$$

where F is applied field and A is a fitting parameter. Since the current is dominated by resonant tunneling current after turn on, we assumed the same trend of equivalent electron mobility from mesh point i to j. It should be pointed that the non-local mobility μ_n and non-local MFP λ_n do not have their usual meaning within the framework of classic transport theory.

2 Simulation results and discussion

The structure studied here is a three-well vertical transition active region QCL with $In_{0.53}Ga_{0.47}As/Al_{0.48}In_{0.52}As$ multiple quantum wells lattice matched to InP and designed for emission at 8 μm. Specific details and experimental results can be found in Ref. 17.

With the transport model shown in section 2, we computed the *J-V* characteristics of QCL at differ-

ent temperature and compared with experimental data. Fig. 1 shows both calculated and experimental *J-V* curves of QCL at 100 K and 425 K, respectively. Excellent agreement can be seen with the fitting parameters shown in Table 1. γ is the broadening of state which is usually a few of milli-electron volts[18-19]. Effective threshold field (F_{th}) is used to effectively describe the current threshold of QCLs. At low temperature, the field is comparable with the resonant field. At high temperature, however, there will be some additional leakage paths, for example, thermionic emission into the active region states, into the continuum and scattering into indirect valley states within the band structure[20], so the effective threshold field will decrease. Non-local mobility (μ_n) and MFP (λ_n) are the fitting parameters which are proportional to the number of periods in QCLs since one-dimensional density of states is proportional to the period number of a QCL[13]. Mobility factor (f_μ) and MFP factor (f_λ) are defined as the effective mobility and MFP per period. The actual non-local mobility and MFP used in calculation is $\mu_n = Nf_\mu\mu$ and $\lambda_n = Nf_\lambda$, respectively, where μ is the normalized non-local mobility computed from Eq. 6 (see Fig. 2).

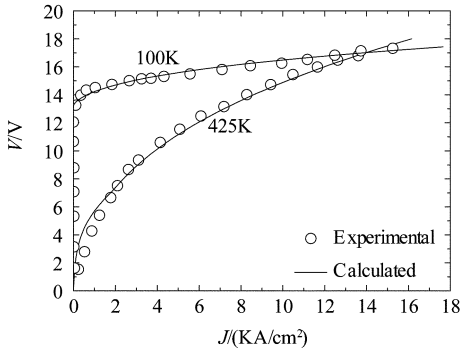

Fig. 1 Calculated and experimental *J-V* curves of the three-well active region QCL at 100 K and 425 K
图1 在100 K和425 K条件下,三量子阱有源区量子级联激光器计算结果与实验结果的对照

Figure 2 shows that non-local mobility reaches a peak at the effective threshold field. At low temperature, only the tunneling path from the injector ground state to the upper laser state is expected to significantly contribute to the current. So the effective threshold field is equivalent to resonant field as shown in Fig. 3 (a). At high temperature, the effective of additional paths can not be ignored, so the device will turn on before resonant, as shown in Fig. 3(b). Broadening of the state is set to be 2 meV and 5 meV at 100 K and 425 K, respectively, so the slope of the non-local mobility at 100 K is much larger than that at 425 K, corresponding to the different differential resistance at different temperature as shown in Fig. 1.

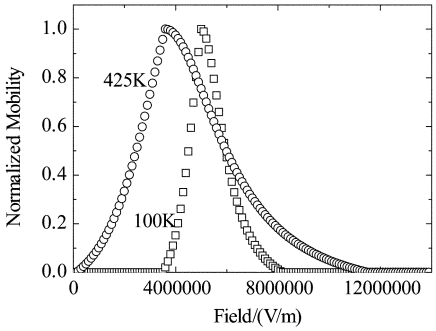

Fig. 2 Normalized non-local mobility at 100 K (open squares) and 425 K (open circles) for the three-well active region QCL
图2 在100 K和425 K条件下,三量子阱有源区量子级联激光器的归一化非局域电子迁移率

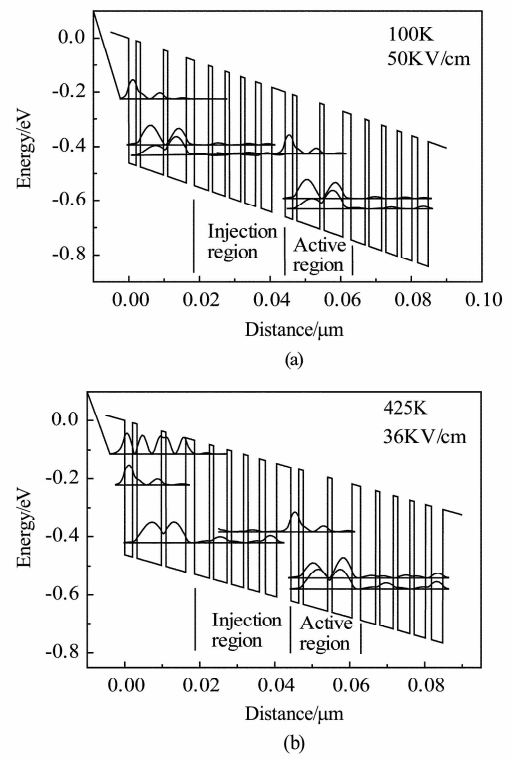

Fig. 3 Conduction band diagram and sub-bands involved in lasing transition in two periods of active/injector region (a) 100 K and, (b) 425 K
图3 两组有源区/注入区多量子阱结构的导带结构图以及导带中参与激光跃迁的子能级的分布图(a)100K,(b)425K

Table 1　Fitting parameters for three-well active region QCL

表 1　三量子阱有源区量子级联激光器的拟合参数

T/K	γ /meV	F_{th}/(V/m)	f_μ/(cm^2/V·s)	f_λ/μm
100	2	5.00E+06	1	0.003
425	5	3.60E+06	0.47	0.0015

To give a further validation of our transport model, we did another group of simulation based on a four-well active region QCL with $In_{0.66}Ga_{0.34}As/Al_{0.69}In_{0.31}As$ and designed for emission at 4.6 μm[21]. With fitting parameters shown in table II, a reasonable agreement is found at both 80 K and 300 K, as shown in Fig. 4. Field dependent mobility calculated from Eq. 6 is shown in Fig. 5. All the fitting parameters have the same trend of the three-well active QCL shown above.

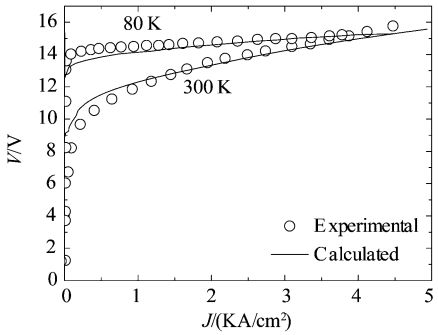

Fig. 4　Calculated and experimental *J-V* curves of the four-well active region QCL at 80 K and 300 K

图 4　在 80 K 和 300 K 条件下,四量子阱有源区量子级联激光器计算结果与实验结果的对照

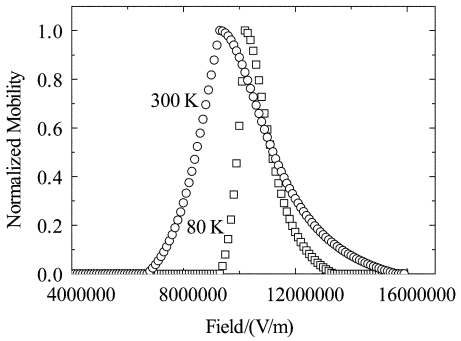

Fig. 5　Normalized non-local mobility to account for long-range carrier transport at 300 K (open circles) and 80 K (open squares) for a four-well active region QCL

图 5　在 80K 和 300K 条件下,四量子阱有源区量子级联激光器的归一化非局域电子迁移率

Table 2　Fitting parameters for four-well active region QCL

表 2　四量子阱有源区量子级联激光器的拟合参数

T/K	γ/meV	F_{th}/(V/m)	f_μ/(cm^2/V·s)	f_λ/μm
80	2	10.2E+06	3.14	0.0084
300	4	9.3E+06	1.16	0.0029

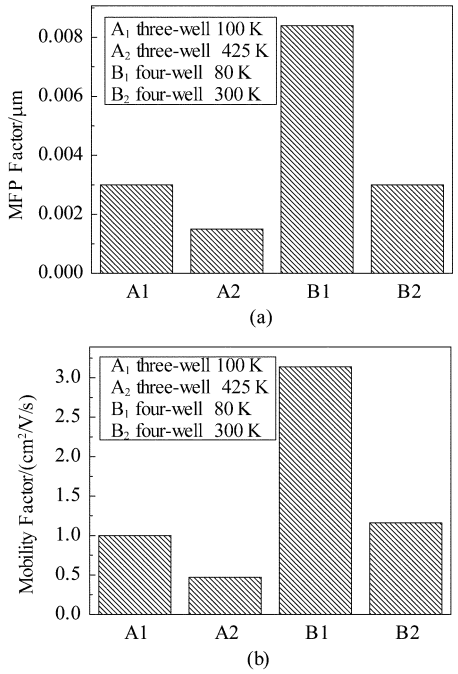

Fig. 6　(a) Non-local MFP factor, and (b) mobility factor for QCLs with different structures at different temperatures

图 6　在不同温度下,不同结构量子级联激光器的(a)非局域平均自由程因子,(b)非局域迁移率因子

We can see from Fig. 6 that non-local MFP factor and mobility factor at high temperature are lower than those at low temperature since carriers will be scattered more easily at higher temperature. Figure 6 also shows that MFP factor and mobility factor of structure B are much larger than those of structure A. It can be explained that the thin barrier-well pair added in the four-well active region in structure B had improved the coupling between ground level of injection and upper laser level. According to Eq. 6, the factors of structure B should be larger than those of structure A.

3　Conclusions

We have presented a simulation study of transport properties of QCLs at different temperature based on non - local transport model . The most important issue

in simulation is the values of fitting parameters, including broadening of state (γ), effective threshold field (F_{th}), non-local mobility factor (f_μ) and non-local MFP factor (f_λ). γ will increase with temperature while mobility and MFP factors will decrease with temperature. With reasonable values of fitting parameters, good agreements have been obtained for QCLs with different structures at different temperature. Although we have a few fitting parameters in our model, the present non-local transport model is still one of the most promising models to predict the transport characteristics in QCLs or other structures with hundreds of barriers, such as quantum well infrared photodetectors (QWIPs) and type II superlattice photodetectors.

REFERENCES

[1] Donovan K, Harrison P, Kelsall R W. Self-consistent solutions to the intersubband rate equations in quantum cascade lasers: Analysis of a GaAs/$Al_xGa_{1-x}As$ device [J]. *J. Appl. Phys.*, 2001, **89**(6): 3084-3090.

[2] Indjin D, Harrison P, Kelsall R W, *et al*. Self-consistent scattering theory of transport and output characteristics of quantum cascade lasers [J]. *J. Appl. Phys.*, 2002, **91**(11): 9019-9026.

[3] Kim J, Lerttamrab M, Chuang S L, *et al*. Theoretical and experimental study of optical gain and linewidth enhancement factor of type-I quantum-cascade lasers [J]. *IEEE J. Quantum Electron.*, 2004, **40**(12): 1663-1674.

[4] Iotti R C, Rossi F. Microscopic theory of hot-carrier relaxation in semiconductor-based quantum-cascade lasers [J]. *Appl. Phys. Lett.*, 2000, **76**(16): 2265-2267.

[5] Iotti R C Rossi F. Nature of charge transport in quantum-cascade lasers [J]. Phys. Rev. Lett., 2001, **87**(14): 146603.

[6] Compagnone F, Carlo A D, Lugli P. Monte Carlo simulation of electron dynamics in superlattice quantum cascade lasers [J]. *Appl. Phys. Lett.*, 2002, **80**(6): 920-922.

[7] Bellotti E, Driscoll K, Moustakas T D, *et al*. Monte Carlo simulation of terahertz quantum cascade laser structures based on wide-bandgap semiconductors [J]. *J. Appl. Phys.*, 2009, **105**(11): 113103.

[8] Wacker A. Gain in quantum cascade lasers and superlattices: A quantum transport theory [J]. *Phys. Rev. B*, 2002, **66**(8): 085326.

[9] Yasuda H, Kubis T, Vogl P, *et al*. Nonequilibrium Green's function calculation for four-level scheme terahertz quantum cascade lasers [J]. *Appl. Phys. Lett.*, 2009, **94**(15): 151109.

[10] Kubis T, Yeh C, Vogl P, *et al*. Theory of nonequilibrium quantum transport and energy dissipation in terahertz quantum cascade lasers [J]. *Phys. Rev. B*, 2009, **79**(19), 195323.

[11] Terazzi R, Gresch T, Wittmann A, *et al*. Sequential resonant tunneling in quantum cascade lasers [J]. *Phys. Rev. B*, 2008, **78**(15): 155328.

[12] Terazzi R, Faist J. A density matrix model of transport and radiation in quantum cascade lasers [J]. *New J. Phys.*, 2010, **12**(03): 033045.

[13] Li Z M Simon, Li Y Y, Ru G. P. Simulation of quantum cascade lasers [J]. *J. Appl. Phys.*, 2011, **110**(09): 093109.

[14] Li Y Y, Ru G P, Li Z M Simon [C]. In *IEEE 9th International Conference on ASIC*, Xiamen, China, Oct. 25-28, 2011: 866-869.

[15] See http://crosslight.com for information about LASTIP and PICS3D simulation software packages.

[16] Ashcroft N W, Mermin N D. *Solid State Physics* [M]. Saunders College Publishing. 1976: 1-28.

[17] Gmachl C, Tredicucci A, Capasso F, *et al*. High-power gimel approximate to 8 (m quantum cascade lasers with near optimum performance [J]. *Appl. Phys. Lett.*, 1998, **72**(24): 3130-3132.

[18] Scalari G, Terazzi R, Giovannini M, *et al*. Population inversion by resonant tunneling in quantum wells [J]. *Appl. Phys. Lett.*, 2007, **91**(3): 032103.

[19] Sirtori C, Capasso F, Faist J, *et al*. Resonant tunneling in quantum cascade lasers [J]. *IEEE J. Quantum Electron.*, 1998, **34**(9): 1722-1729.

[20] Pflugl C, Diehl L, Lyakh A, *et al*. Activation energy study of electron transport in high performance short wavelengths quantum cascade lasers [J]. *Opt. Express*, 2010, **18**(2): 746-753.

[21] Liu P Q, Hoffman A J, Escarra M D. Highly power-efficient quantum cascade lasers [J]. *Nature Photon.*, 2010, **4**: 95-98.